

Secretome of the Free-living Mycelium from the Ectomycorrhizal Basidiomycete *Laccaria bicolor*

Delphine Vincent,^{*,†} Annegret Kohler,[‡] Stephane Claverol,[§] Emilie Solier,[§] Johann Joets,^{||} Julien Gibon,[‡] Marc-Henri Lebrun,[⊥] Christophe Plomion,^{*,†} and Francis Martin^{*,‡}

[†]INRA, UMR1202 BIOGECO, Cestas, France

[‡]INRA, UMR1136 Interactions Arbres/Micro-Organismes, Nancy, France

[§]Plate-forme Protéomique, Université Bordeaux 2, Bordeaux, France

^{||}UMR Génétique Végétale du Moulon, Gif-sur-Yvette, France

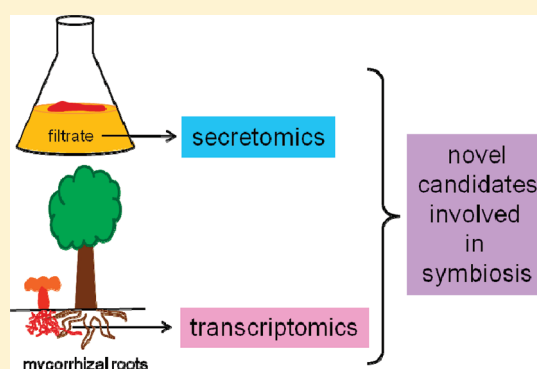
[⊥]CNRS, Bayercropscience, UMR 2847, Lyon, France

S Supporting Information

ABSTRACT: The ectomycorrhizal basidiomycete *Laccaria bicolor* has a dual lifestyle with a transitory soil saprotrophic phase and a longer mutualistic interaction with tree roots. Recent evidence suggests that secreted proteins play key roles in host plant colonisation and symbiosis development. However, a limited number of secreted proteins have been characterized, and the full spectrum of effectors involved in the mycobiont invasion and survival remains unknown. We analyzed the extracellular proteins secreted in growth medium by free-living mycelium of *L. bicolor* as a proxy for its saprotrophic phase. The proteomic analyses (two-dimensional electrophoresis and shotgun proteomics) were substantiated by whole-genome expression transcript profiling on ectomycorrhizal roots. Among the 224 proteins identified were carbohydrate-acting enzymes likely involved in the cell wall remodelling linked to hyphal growth as well as

secreted proteases possibly digesting soil organic compounds and/or fending off competitors, pathogens, and predators. Evidence of gene expression was found in ectomycorrhizal roots for 210 of them. These findings provide the first global view of the secretome of a mutualistic symbiont and shed some light on the mechanisms controlling cell wall remodelling during the hyphal growth. They also revealed many novel putative secreted proteins of unknown function, including one mycorrhiza-induced small secreted protein.

KEYWORDS: 2-DE, ectomycorrhizal fungus, *Laccaria bicolor*, mycelium, secreted proteins, secretomic, shotgun proteomics, symbiosis



1. INTRODUCTION

Ectomycorrhizal (ECM) fungi colonize the dominant tree species (e.g., birch, poplar, beech, eucalypt, pine trees) in temperate and boreal forests where they have a beneficial impact on plant growth in natural and agroforestry ecosystems and allow the completion of the fungal life cycle.¹ In addition to supplying water at the fungal–plant cell interface, the mutualistic fungi actively transfer nutrients to the plant. In return for 10–20% of photosynthetically derived sugars, ectomycorrhizal fungi supply 70% of the plant's nitrogen and phosphorus needs.² The first step in the establishment of the ECM symbiosis is attachment to and colonisation of lateral roots by a compatible fungal mycelium. While only a few of the chemical cues that control recognition between ECM fungi and their host plants have been identified,^{3,4} the early morphological stages of ECM colonization have been well characterized in a number of systems⁵ and it is understood that symbiosis development requires specific cell–cell and cell–substrate interactions that direct the extension of hyphae to their precise host root targets. Role of fungal cell walls (CW)

and the extracellular matrix in ECM development is supported by the observed alterations in composition upon the infection process and the subsequent formation of the symbiotic interface.^{5–7} These changes are likely controlled by a tight regulation of the balance between the synthetic and degradative pathways for the polymers that constitute the CW and by the directed and targeted secretion of both enzymes and CW components to sites of the fungal–host interfaces. Proteins that are secreted from hyphae into the extracellular matrix of the symbiotic interface are also probably involved in intercellular and interorganismal communication. This group of proteins is referred to as the fungal secretome.

Among these secreted proteins are proteins involved in adhesion, communication and hydrolysis of CW and substrate

Special Issue: Microbial and Plant Proteomics

Received: September 6, 2011

polymers. Adhesion to the root during formation of the mycorrhizal mantle is achieved through fungal secretion of oriented fibrillar materials that contain polysaccharides, glycoprotein mucigel, and hydrophobins.⁶ Once the mantle is formed and hyphae reach the epidermal cells, the fungus secretes a cocktail of CW modifying proteins, such as expansins and carbohydrate-active enzymes⁸ and various polysaccharides (chitosans and β -1,3-glucans).⁷ Although loss of CW degrading enzymes is a characteristic feature of ECM fungi,^{9,10} it has mainly reduced the number of plant CW-modifying or -degrading enzymes (e.g., GH6 and GH7 cellulases), without completely eliminating all such genes. A small contingent of carbohydrate-active enzymes (CAZymes) remains, sufficient to aid penetration of fungal hyphae between root cells but unlikely able to use the root cells as a nutrient source. These proteins may act to loosen contact between root cells so that fungal hyphae can penetrate between the epidermal root cells without destruction or penetration of the plant cell.¹¹

The 65-Mb haploid genome of the most intensively studied ECM fungus, *Laccaria bicolor*, has been sequenced by the U.S. Department of Energy's Joint Genome Institute. Analysis of the draft genome⁸ and substantially improved assembly and gene models (<http://genome.jgi-psf.org/Lacbi2/Lacbi2.home.html>) revealed many genes potentially coding for secreted proteins. Out of the 2931 proteins predicted to be secreted by *L. bicolor*, most (67%) cannot be ascribed a function, and 82% of these predicted proteins are specific to *L. bicolor*. Within this set, a large number of genes encode cysteine-rich products that have a predicted size of <300 amino acids. An increasing body of evidence revealed that several of these small secreted proteins (SSPs) are key effectors mediating the interactions between the ECM fungus *Laccaria bicolor* and its hosts.^{10,12} The Mycorrhizal Induced Small Secreted Protein 7 (MiSSP7), the most highly symbiosis-up-regulated gene from *L. bicolor*,⁸ encodes an effector protein required for the establishment of the ECM symbiosis. MiSSP7 is secreted by the fungus upon receipt of diffusible signals from plant roots, imported into the plant cell via phosphatidylinositol 3-phosphate-mediated endocytosis, and targeted to the plant nucleus where it alters the transcriptome of the plant cell. *L. bicolor* transformants with reduced expression of MiSSP7 do not develop symbiosis with poplar roots.¹² These investigations support the importance of SSPs in the development of the mycorrhizal symbiosis, but considerable uncertainty persists with respect to the roles and interactions of hundreds of genes coding for oxidative and hydrolytic enzymes during the different developmental stages of *L. bicolor*. In addition, only a limited number of predicted secretory proteins have been characterized at the proteomic level to date. Although many of the putative secreted proteins may be retained in internal compartments such as the endoplasmic reticulum (ER) or secretory pathways, a significant fraction is probably exported to external sites for interaction with the host plant.

The coupling of high resolution protein separation techniques, such as two-dimensional electrophoresis (2-DE), with high throughput identification strategies has allowed the large scale analysis of protein identity and expression in several fungal systems (see ref 13 for review). The completion of the genome of *L. bicolor*⁸ allows for examination of secreted proteins released by the ECM symbiont. Here we combined transcriptome analyses of predicted secreted proteins and mass spectrometric (MS) identification of extracellular proteins to characterize the secretome of the free-living mycelium (FLM) of *L. bicolor* grown on synthetic growth medium (as a proxy for the saprotrophic

mycelium). Our findings revealed that *L. bicolor* mobilizes a rich repertoire of enzymes potentially involved in nutrient acquisition, and a series of hypothetical proteins with unknown function, including mycorrhiza-induced small secreted proteins (MiSSPs).

2. MATERIALS AND METHODS

L. bicolor culture, sampling and processing are described in.¹⁴ Briefly, mycelium of *L. bicolor* strain S238N-H82 was grown with shaking in 1 L Erlenmeyers filled with 500 mL Pachlewski medium¹⁵ (see Supporting Information for composition). After five weeks of growth at 25 °C, the liquid medium containing the secreted proteins was filtered with filter paper and then frozen at -80 °C. The mycelium was immediately frozen in liquid nitrogen.

2.1. Protein Separation

An outline of the three separation techniques used in this study is presented in Figure 1.

2.1.1. IPG-IEF Shotgun. A lyophilized secretome protein sample (0.2 g) was resuspended in 0.5 mL of 50 mM ammonium bicarbonate (pH 8) and 20 μ L of 2 M DTT. Then trypsin (demethylated, proteomics grade, Sigma, Lyon, France) diluted in 50 μ L of HCl (10 μ g/mL) was added and left for incubation at 37 °C overnight. Tryptic peptides were completely dehydrated in a vacuum centrifuge and resuspended in 8 M urea, 1% (w/v) DTT and 1% (v/v) pH 3.5–5 CAs. IPG-IEF shotgun proteomics was performed on the tryptic mixture using a 18 cm pH 3.5–4.5 IPG DryStrip (GE Healthcare, Uppsala, Sweden) as described in ref 16, except that the IPG strip was cut into 40 fractions instead of 43. Tryptic peptides were eluted from the strip fractions using C18 ZipTip columns (Sep-Pak C18 MicroElution Plate, Waters SAS, Milford, MA). IPG fractions were kept at -20 °C until MS analyses.

2.1.2. SDS-PAGE Shotgun. SDS-PAGE was performed according to¹⁷ using the MG-202 model mini-gel system (CBS Scientific CO., Del Mar, CA), by loading 0.2 g of proteins from mycelium and secretome samples in separate lanes of the 11% polyacrylamide gel. Each lane was cut into 16 fractions (Supplementary Figure S1, Supporting Information). The SDS-PAGE fractions were kept at -20 °C until trypsin digestion prior to MS analyses.

2.1.3. 2-DE. 2-DE¹⁸ was performed using IPG-IEF in the first dimension (24 cm) and SDS-PAGE in the second dimension (11% polyacrylamide gel). IEF was conducted using 24 cm IPG strips (Immobiline DryStrip, GE Healthcare) of various pH ranges (3–11NL, 4–7 and 7–11NL) by loading 0.2 g of proteins from both mycelium and secretome samples. 2-D gels were produced as indicated in.¹⁴ Full details are provided in the Supporting Information.

Both 1- and 2-D gels were stained using the silver staining procedure compatible with MS analyses edited by Virginia Tech Center for Genomics (<http://vigen.biochem.vt.edu/protocols/AgStain.pdf>). Gel images were digitalized using ImageScanner (model UTA III, GE Healthcare) and 2-D images were analyzed using Progenesis PG240 software (Nonlinear Dynamics Ltd., Newcastle upon Tyne, U.K.). Images of 2-D gels are provided in Supplementary Figure S2 (Supporting Information). The most abundant spots were manually excised from 2-D gels, in duplicate or triplicate whenever possible. Thus 75 spots from 4 to 7 patterns using mycelium samples were excised prior to MS analyses; for the secretome analysis, 134 spots from 3 to 11

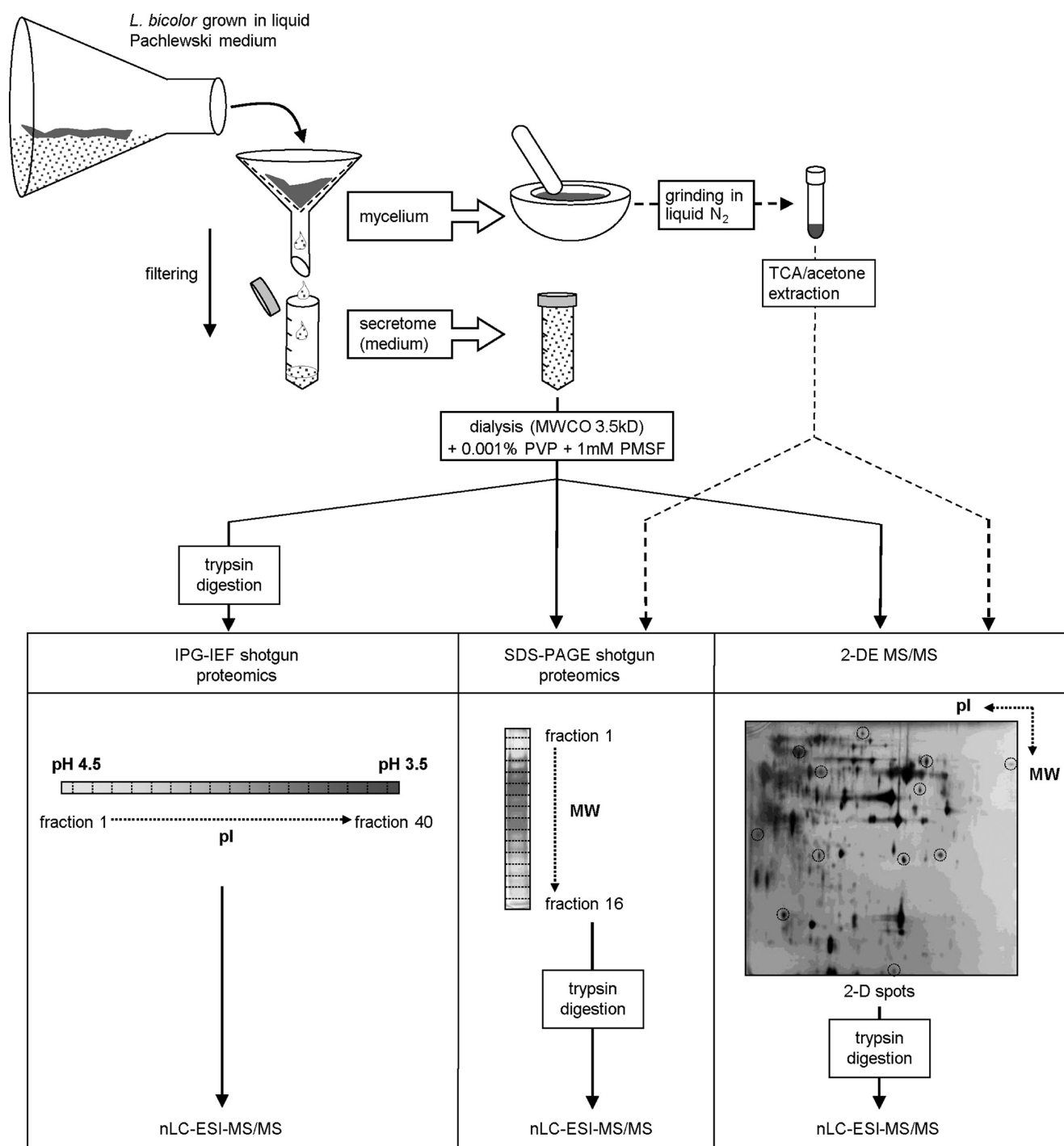


Figure 1. Outlines of the three resolving proteomic methods used to separate and identify *L. bicolor* proteins.

NL patterns, 46 spots from 4 to 7 patterns, and 21 spots from 7 to 11NL patterns were excised. Excised spots were processed as indicated in ref 14.

2.2. Protein Identification by MS/MS

Trypsin digestion of proteins contained in SDS-PAGE fractions and 2-D spots was performed as in ref 14. It is fully described in the Supporting Information.

The peptide mixture was analyzed by online capillary HPLC (LC Packings, Amsterdam, The Netherlands) coupled to a nanospray

LCQIT mass spectrometer (Thermo-Finnigan, San Jose, CA) for 2-D spots and a nanospray LTQIT mass spectrometer (Thermo-Finnigan) for IPG strip and SDS-PAGE fractions. Ten microliters of peptide digests were loaded onto a 300- μm \times 5-mm C18 PepMap trap column (LC Packings) at a flow rate of 30 $\mu\text{L}/\text{min}$. The peptides were eluted from the trap column onto an analytical 75- μm id \times 15-cm C18 PepMap column (LC Packings) with a 5–40% linear gradient of solvent B in 35 min (solvent A was 0.1% (v/v) HCOOH in 5% (v/v) ACN, and solvent B was 0.1% (v/v) HCOOH in 80% (v/v) ACN). The separation flow rate

was set to 200 nL/min. The mass spectrometer operated in positive ion mode at a 2-kV needle voltage and a 3-V capillary voltage. Data were acquired in a data-dependent mode alternating a MS scan survey over the range m/z 300–1700 and three MS/MS scans in an exclusion dynamic mode. MS/MS spectra were acquired using a 2 m/z unit ion isolation window, 35% relative collision energy, and 0.5 min dynamic exclusion duration.

2.3. Database Search

Peptide sequences were queried against the predicted protein sequences of *L. bicolor* v1.0 available at the JGI (BestModels v1.0, release date March 10, 2008, <http://genome.jgi-psf.org/Lacbi1/Lacbi1.home.html>). Protein sequences from keratin and trypsin were also included during the searching process; they were downloaded from UniProtKB/Swiss-Prot (Release 55.2, 335 entries). Data were searched by SEQUEST through Bioworks 3.3.1 interface (ThermoFinnigan). Parameters used are indicated in¹⁴ and fully described in the Supporting Information. All protein identifications were based on a minimum of two peptide assignments for 2-D spots analyses and a minimum of one peptide for shotgun analyses. For the latter, the False Positive Rate (FPR) was estimated by searching against a reversed decoy database. The FPR obtained was 1.9%. Notably, no false positives were detected with more stringent criteria (i.e., limit of 2 peptides minimum).

Identities of secreted proteins are summarized in Table 1. Summaries of protein identifications per method using numbers of identified proteins and gene ontology terms are presented in Supplementary Tables S1 and S2, respectively (Supporting Information). All MS details pertaining to the analysis of both secreted and mycelial proteins are included in Supplementary Tables S3 and S4 (Supporting Information). Two-dimensional patterns, with detected and excised 2-D spots, as well as MS results from both mycelium and secretome samples were uploaded to the PROTEOME database;¹⁹ they can be viewed at http://proteus.moulon.inra.fr/proticbiogeco/web_view/index.php.

2.4. Bioinformatics

To estimate how appropriate 2-DE was to resolve secreted proteins from *L. bicolor*, we computed both theoretical pIs and MWs of all the predicted proteins and then established the coverage given by our electrophoretic conditions. Theoretical pIs and MWs were obtained by using the online ExPASy compute pI/MW tool²⁰ (http://www.expasy.org/tools/pi_tool.html). Results are graphically illustrated in Supplementary Figure S3 (Supporting Information). For a more in depth assessment, we limited such an analysis to proteins that were predicted to be secreted and computed the percentage covered by our electrophoretic conditions. The TargetP algorithm²¹ (<http://www.cbs.dtu.dk/services/TargetP/>) was used online to predict targeted compartments (see parameters in Supporting Information).

Protein sequences that were not manually annotated at the JGI *L. bicolor* portal were annotated using UniProtKB (<http://www.uniprot.org/>) and the BLASTP algorithm²² (<http://blast.ncbi.nlm.nih.gov/Blast.cgi>) searching first the SwissProt (SP) database, then the NCBI non redundant (nr) database when no annotation was retrieved using SP. This was performed through the Blast2GO (B2G) interface (<http://www.blast2go.de/>) which retrieved E.C. numbers and Gene Ontology (GO, <http://www.geneontology.org/>) terms (Table 1 and Supplementary Table S5, Supporting Information). The CAZY database²³ (<http://www.cazy.org/>) was also searched.

Protein annotations, E.C. numbers, GO terms, theoretical pIs and MWs, and TargetP location predictions are indicated in Table 1.

2.5. Transcript Profiling

The *Laccaria bicolor* custom-exon expression array version 2 ($4 \times 72K$) manufactured by Roche NimbleGen Systems Limited (Madison, WI) (<http://www.nimblegen.com/products/exp/index.html>) contained three independent, nonidentical, 60-mer probes per gene model. For 18,653 annotated protein-coding gene models from the *L. bicolor* genome v1 (<http://genome.jgi-psf.org/Lacbi1/Lacbi1.home.html>) probes could be designed. Included in the array were 2,032 random 60-mer control probes and labeling controls. Three biological replicates were used for each microarray experiments. For 4,702 probes, technical duplicates were included on the array. Full details of the transcript profiling can be found in the Supporting Information. Transcript abundances corresponding to the genes encoding for *L. bicolor* secreted proteins are listed in Table 1.

3. RESULTS

3.1. Protein Identification from the Free-living Mycelium (FLM)

Two methods were employed to identify mycelial proteins: SDS-PAGE shotgun and 2-DE-MS/MS. The SDS-PAGE shotgun method yielded 1616 proteins in total across all 16 fractions, accounting for 815 unique accessions when duplicates are removed (Supplementary Table S1, Supporting Information). Four proteins were found in all 16 fractions (one enolase and 3 glyceraldehyde 3-phosphate dehydrogenases, GAPDH), all of them involved in glycolysis and known to be extremely abundant in fungi.²⁴ We hypothesize that those highly prominent proteins both form supercomplexes and undergo proteolysis thereby achieving a MW continuum. Mycelial proteins were also separated using 2-DE, along various pH ranges. A total of 1104, 1379, and 272 spots were resolved along 3–11, 4–7 and 7–11NL pH gradients, respectively (Supplementary Figure S2, Supporting Information). Using the *L. bicolor* gene repertoire, we computed both theoretical pIs and MWs for all sequenced proteins. It must be noted that such computation does not consider post-translational modifications (PTMs), which usually account for most pI and MW variations. Interestingly, a spot-depletion area was visible at neutral pIs (7.3), thus creating a bimodal distribution (black dots in Supplementary Figure S3, Supporting Information). Such bimodality has recently been reported across all taxa.^{25,26} This distribution suggests that alkaline and acidic proteins are equally represented in *L. bicolor*. This was not congruent with the 2-D patterns of the mycelium (Supplementary Figures 2C and E, and purple dots in Supplementary Figure 3B, Supporting Information), displaying five time more acidic than alkaline proteins. However, alkaline proteins are known to be particularly difficult to extract and separate using 2-DE without any specific procedure.²⁷ Similar results were observed for the ascomycete *Leptosphaeria maculans*.¹⁴ The 75 most abundant protein spots were analyzed by MS and matched to their cognate genes using BLAST algorithm. They yielded a total of 316 proteins, most of them redundant (52%) since only 163 unique accessions were identified. Consistent with the SDS-PAGE shotgun analysis, enolase was again predominant, being identified in 11 spots. For each MS run, the complete set of peptide tandem mass spectra was submitted to SEQUEST for protein sequence

Table 1. List of *Laccaria bicolor* Secreted Proteins Identified by the Three Methods and Annotated (sorted by code), along with Evidence of Gene Expression (2.5-fold change highlighted in green when down-regulated and red when up-regulated), 2-fold change highlighted in light green when down-regulated and orange when up-regulated) in Free-living Mycelium (FLM) and Ectomycorrhiza (ECM) Roots of Douglas fir, *Populus trichocarpa* and *Populus deltoides*

protein ID	method	code*	description (amotations retrieved from UniProtKB, JGI manual, or JGI automatic)	SP/Inr	EC number	GO BP	GO MF	GO CC	TargetP location*	Theor. pI/MW	FLM	Douglas fir ECM	P. Tricho ECM	P. delto ECM
323411	IPG	1433	14-3-3 protein			signal transduction	protein binding	cytoplasm	-	5.61/13.88	42312	49235	38912	49276
295281	1D	ACMSD	Aminocarbonylmucronate-semialdehyde decarboxylase		4.1.1.45	unknown process	unknown function	unknown compartment	-	5.94/20.07	13288	5431	4445	4238
145093	2D	ACT	Actin			CCOOB	protein binding	cytoplasm	-	5.10/41.30				
192701	2D	ACT	Actin			CCOOB	protein binding	cytoplasm	-	5.05/53.38	47022	49121	44482	49705
303955	IPG	ALF	Fructose-bisphosphate aldolase		4.1.2.13	CM	actin binding	intracellular	-	N.A.	39254	18179	23357	
288151	IPG	ANK	Ankyrin			endocytosis	transferase activity	golgi apparatus	-	5.95/54.01	4537	1072	646	227
310440	IPG	ARF	ARF GTPase activator, putative			unknown process	ion binding	cytoplasm	-	6.28/41.17	133	541	11952	10702
305432	IPG/1D	ATPa	H ⁺ -transporting two-sector ATPase, alpha/beta subunit		3.6.3.14	ATP biosynthesis	ATP binding	membrane	M	9.36/60.68	44194	29209	27211	27132
306417	IPG	ATPase	AAA-ATPase		3.6.4.-	ATP biosynthesis	ATP binding	mitochondrion	M	5.68/37.11	2334	1159	1192	1293
313946	IPG	ATPb	H ⁺ -transporting two-sector ATPase, delta subunit		3.6.3.14	ATP biosynthesis	ATP binding	membrane	M	5.78/48.48	47932	39809	32536	32458
296236	IPG	BSD	Bsd domain-containing protein 1			unknown process	unknown function	cytoplasm	-	6.57/70.40	10104	4791	4135	4877
243722	IPG	CALX	Calnexin			ion transport	ion binding	endoplasmic reticulum	-	5.63/60.96	47585	37973	44442	41000
318727	1D	CCPI	Citrocyin cysteine proteinase inhibitor			PI/MTT	protein binding	extracellular	-	5.59/52.79	1562	28843	46849	28244
157859	2D	CDH	Choline dehydrogenase		1.1.99.1	electron transport	oxidoreductase activity	membrane	-	10.01/28.72	39717	3404	1112	1478
182815	1D/2D	CE10	Carotenoid esterase		N.A.	lipid metabolism	hydrolase activity	extracellular	S	8.31/11.61	12203	857	255	181
306103	IPG/1D/2D	CE10	Carotenoid esterase		3.1.1.1	unknown process	unknown function	extracellular	S	9.97/20.23	8945	7944	5613	2875
315843	2D	CE10	Carotenoid ester lipase		N.A.	lipid metabolism	hydrolase activity	intracellular	S	6.19/34.51	1463	3551	1527	1452
152235	1D/2D	CE4	Chitin deacetylase		3.5.1.41	CCOOB	hydrolase activity	unknown compartment	S	6.05/18.55	36734	21111	16743	20053
229432	IPG/1D/2D	CE4	Chitin deacetylase		3.5.1.41	CCOOB	hydrolase activity	unknown compartment	S	7.71/22.25	27919	15379	16890	16304
253995	IPG/2D	CE4	Chitin deacetylase		3.5.1.41	CCOOB	hydrolase activity	unknown compartment	S	6.68/83.91	21865	12205	9144	10690
253920	IPG	CE4	Chitin deacetylase		3.5.1.41	CCOOB	hydrolase activity	unknown compartment	S	8.75/27.89	31707	884	438	268
293318	1D	CE4	Chitin deacetylase		3.5.1.41	CCOOB	hydrolase activity	unknown compartment	S	8.80/39.13	5832	6687	9045	9244
307596	2D	CE4	Chitin deacetylase		3.5.1.41	CCOOB	hydrolase activity	unknown compartment	S	9.35/10.82	47863	15733	1241	1961
245373	IPG/1D/2D	CE8	Pectinesterase		3.1.1.11	CWOB	hydrolase activity	cell wall	S	8.31/59.22	13235	3759	8225	7399
316460	IPG	CE9c	N-acetylglucosamine-6-phosphate deacetylase		3.5.1.25	CM	hydrolase activity	unknown compartment	S	5.98/113.57	16040	3740	1945	2174
233639	IPG/1D/2D	CP1c1	Concanamycin induced protein c1			unknown process	unknown function	unknown compartment	-	5.58/38.55				
190553	1D	COX12	Cytochrome c oxidase, subunit Vlb		1.9.3.1	electron transport	oxidoreductase activity	mitochondrion	-	6.41/38.21	34693	26788	23011	23878
173909	IPG	COX4	Cytochrome c oxidase, subunit Vlb		1.9.3.1	electron transport	oxidoreductase activity	mitochondrion	M	9.28/103.35	36802	28019	21367	22853
292906	2D	CPEFS	Candidapepsin		3.4.23.24	PI/MTT	protein binding	extracellular	S	N.A.	58218	53657	43696	44762
172945	1D	CPSP	Cerato-platanin-related secreted protein			response to stress	unknown function	unknown compartment	S	8.84/13.65	1677	698	900	343
240888	IPG	CTb5	Cytochrome b5			electron transport	electron carrier activity	mitochondrion	-	8.25/62.12	41326	41142	30073	41455
191797	1D	CY12	Ubiquinol-cyt C reductase complex core protein 2			electron transport	electron carrier activity	mitochondrion	M	8.35/61.56	19365	8883	5659	7043
315088	IPG	DDR48	DNA damage-responsive protein 48			response to stress	ATP binding	cytoplasm	-	8.40/71.27	30217	4992	11569	
248920	IPG	DF1G	Elongation factor 1-gamma			PI/MTT	protein binding	cytoplasm	-	9.19/49.03	55188	44098	25882	34668
292544	IPG	ENDOS	GAMP-regulated phosphoprotein/endo-sulfine			unknown process	unknown function	unknown compartment	-	9.98/8.47	27726	36941	35748	36496
181287	IPG/1D/2D	ENO	Enolase		4.2.1.11	CM	RNA binding	cell wall	-	9.62/12.79	46247	45607	51363	48035
301440	1D	ERN	Endonuclease L-PSP		3.1.26.-	CM	RNA binding	nucleus	-	10.28/34.13	10529	16360	21757	29797
243925	1D	EXPN	Expansin Family protein			CCOOB	hydrolase activity	cytoplasm	M	7.42/47.98	35236	20529	14024	16926
185280	IPG	FBRLL	Fibrillin		4.2.1.2	CM	oxidoreductase activity	cytoplasm	-	9.39/25.59	32510	10155	5442	7316
300776	IPG	FUMH	Fumarate hydratase		1.1.3.9	cell adhesion	oxidoreductase activity	unknown compartment	-	8.57/64.22	23372	10547	14727	12433
151504	2D	GAOX	Galactose oxidase		1.1.3.9	cell adhesion	oxidoreductase activity	unknown compartment	S	10.30/10.64	21979	12427	13006	12046
247761	IPG/1D/2D	GAOX	Galactose oxidase		1.1.3.9	cell adhesion	oxidoreductase activity	cytoplasm	-	7.65/37.09	10111	991	670	826
313835	IPG/1D	GAOX	Galactose oxidase		1.1.3.9	CM	dehydrogenase activity	cytoplasm	-	6.89/23.00	49407	21626	17818	25617
184409	1D	GAPDH	Glyceraldehyde 3-phosphate dehydrogenase		1.2.1.-	CM	dehydrogenase activity	cytoplasm	M	9.58/21.69	44686	36335	24489	32010
295504	1D	GAPDH	Glyceraldehyde 3-phosphate dehydrogenase		1.2.1.-	CM	dehydrogenase activity	cytoplasm	-	10.01/27.65	40298	34325	40847	37124
318873	1D	GAPDH	Glyceraldehyde 3-phosphate dehydrogenase		1.2.1.-	CM	dehydrogenase activity	cytoplasm	M	10.01/27.65	40298	34325	40847	37124
294390	1D	GAS1	Gas1-like protein			unknown process	unknown function	unknown compartment	S	10.01/27.65	40298	34325	40847	37124
161487	1D	GH	O-glucosyl hydrolase		N.A.	CM	hydrolase activity	unknown compartment	M	5.28/50.33				
151776	IPG/2D	GH13	Alpha-amylase		3.2.1.1	CM	hydrolase activity	unknown compartment	M	5.23/16.76				
313084	IPG/1D/2D	GH13	Alpha-amylase		3.2.1.1	CM	hydrolase activity	extracellular	S	9.03/58.03	413	1326	3677	3731
295790	IPG	GH15	Glucoan 1,4-alpha-glucosidase		3.2.1.3	CM	carbohydrate binding	unknown compartment	S	8.11/71.73	7832	4327	2660	1460
309096	1D/2D	GH15	Glucoan 1,4-alpha-glucosidase		3.2.1.3	CWOB	carbohydrate binding	cell wall	S	6.62/79.16	16008	4285	494	219
182806	1D	GH16	Endo-1,3(4)-beta-glucanase		3.2.1.6	CWOB	carbohydrate binding	cell wall	S	5.72/28.56	16729	178	492	173
191735	IPG/1D/2D	GH16	Endo-1,3(4)-beta-glucanase		3.2.1.6	CWOB	carbohydrate binding	cell wall	S	5.72/28.56	16729	178	492	173

Table 1. Continued

protein ID	code*	description (annotations retrieved from UniProtKB, JGI manual, or JGI automatic)	SP/Pr, number	E.C. number	GO BPs	GO MF	GO CC	TargetP location*	Theor. pI/MW	FLM	Douglas fir ECI	P. Tricho ECI	P. delto ECI
296997	GH17	Glucan 1,3-beta-glucosidase	3.2.1.58	CWOB	carbohydrate binding	cell wall		S	5.1024,91	27366	28306	31290	36573
323649	GH17	Glucan 1,3-beta-glucosidase	3.2.1.58	CWOB	carbohydrate binding	cell wall		S	7.73950,82	11797	2893	5162	4942
180319	IPG/1D/2D	Chitinase	3.2.1.14	CCOB	hydrolyase activity	unknown compartment		S	9.9732,71	4968	2404	1844	1762
182604	GH20	Beta-N-acetylglucosaminidase	3.2.1.96	CM	hydrolyase activity	cytoplasm		S	8.9156,21	2935	4287	4287	7583
278749	1D/2D	Lysozyme	3.2.1.17	CWOB	hydrolyase activity	extracellular		S	9.4023,23	1713	13607		7259
187145	GH3	Beta-glucosidase	3.2.1.21	CM	hydrolyase activity	unknown compartment		S	5.9620,39	27048			
324539	IPG/1D/2D	Alpha-glucosidase	3.2.1.20	CWOB	carbohydrate binding	cell wall		S	6.6167,92	11357	12649	14705	22988
246054	1D	Acid trehalase	3.2.1.28	CM	hydrolyase activity	cell wall		S	6.6726,47	24977	2443	1737	851
190685	1D	Alpha-mannosidase	3.2.1.113	PM/MT	hydrolyase activity	cytoplasm		S	9.8070,99	44181	18327	14948	23291
305032	GH5	Glucan endo-1,6-beta-glucosidase	3.2.1.75	CWOB	carbohydrate binding	cell wall		S	6.7938,66	39651	29110	4424	45750
143003	IPG/1D/2D	Beta-1,3-glucanotransferase	2.4.1.-	unknown process	transferase activity	intracellular		S	6.4420,58	32999	13297	19883	15582
187145	IPG/1D/2D	Beta-1,3-glucanotransferase	2.4.1.-	unknown process	transferase activity	intracellular		S	9.9838,06	11846	11846	8068	9696
184692	IPG/2D	Beta-glycan active enzyme	3.2.1.-	CM	hydrolyase activity	extracellular		S	5.72118,91	33672	543	268	268
295325	2D	Beta-glycan active enzyme, Laccaria-specific	3.2.1.31	CM	hydrolyase activity	extracellular		S	8.38714,95	23312	1012	821	668
295469	IPG	Beta-glycan active enzyme, Laccaria-specific	3.2.1.31	CM	hydrolyase activity	extracellular		S	5.996,33	36001	17775	10845	13166
190025	IPG	Glycine hydroxymethyltransferase	2.1.2.1	CM	transferase activity	cytoplasm		M	9.8726,51	9330			
314722	IPG/1D/2D	Glucosylsaccharide oxidase	N.A.	unknown process	oxidoreductase activity	unknown compartment		S	6.3396,50	19935			
174286	1D/2D	Glucose oxidase	1.1.3.4	electron transport	oxidoreductase activity	extracellular		S	9.3021,02	8388	6970	12351	12079
308269	1D/2D	GPI-specific phospholipase C	4.6.1.14	lipid metabolism	phospholipase activity	cytoplasm		S	6.20710,38	899	1534	757	1035
318365	1D/2D	GPI-specific phospholipase C	4.6.1.14	lipid metabolism	phospholipase activity	intracellular		S	5.55711,34	4585	1268	1484	2620
336698	1D/2D	GPI-specific phospholipase C	4.6.1.14	lipid metabolism	phospholipase activity	intracellular		S	10.0125,01	122	353	127	69
292424	1D	GPI-SSP		unknown process	unknown function	unknown compartment		S	4.7538,41	552	7464	15008	18879
295228	IPG	GPI-anchored small secreted protein		unknown process	unknown function	unknown compartment		S	8.7668,79	8972	10010	3849	3532
335166	IPG	GPI-anchored small secreted protein		unknown process	unknown function	unknown compartment		S	9.3327,17	1789	2950	2251	3073
336888	IPG	GPI-anchored small secreted protein		unknown process	unknown function	unknown compartment		S	9.6218,53	8872	10010	3849	3532
291682	IPG	Glycogenin glycosyltransferase	2.4.1.-	glycogen biosynthesis	transferase activity	cytoplasm		S	8.5843,22	11809	10885	22682	15984
174455	1D	Histone H4	2.4.1.186	CCOB	DNA binding	nucleus		-	8.9843,32	8989	10885	22682	15984
191132	1D	Histone H4		CCOB	DNA binding	nucleus		-	5.8430,22	7350	16127	28604	25870
191150	1D	Histone H4		CCOB	DNA binding	nucleus		-	6.3545,37	8165	11809	27235	24791
291419	1D	Histone H4		CCOB	DNA binding	nucleus		-	11.36711,37	22258	22258	30574	29581
306722	1D	Histone H4		CCOB	DNA binding	nucleus		-	9.9523,59	1174	1430	7737	16533
186670	1D	Heat shock protein 20 kD		PM/MT	protein binding	cytoplasm		-	7.3170,47	345	761	3892	6084
190797	1D	Heat shock protein 20 kD		PM/MT	protein binding	cytoplasm		-	5.8719,50	104	12	186	876
236684	1D	Heat shock protein 20 kD		PM/MT	protein binding	cytoplasm		-	5.1328,20	194	160	1134	1619
298293	1D	Heat shock protein 20 kD		PM/MT	protein binding	cytoplasm		-	5.9817,86	2924	2633	7569	16079
298306	1D	Heat shock protein 20 kD		PM/MT	protein binding	cytoplasm		-	9.8618,95	28836	23179	37237	36275
189866	IPG/1D	Heat shock protein 90 kD		PM/MT	protein binding	cytoplasm		S	10.5215,97	38656	30005	44436	44436
232979	IPG	Heat shock protein 90 kD		PM/MT	protein binding	cytoplasm		-	8.8535,16	42485	49796	40832	43225
192615	IPG	Eukaryotic initiation factor 5A		PM/MT	protein binding	nucleus		-	5.2717,30	1520	1144	1748	1449
315595	IPG	Inositol polyphosphate kinase	2.7.1.158	phosphate metabolism	ATP binding	cytoplasm		-	8.9820,06	7335	18402	5190	8879
252630	IPG	Voltage-gated potassium channel subunit beta		ion transport	ion binding	mitochondrion		-	4.5623,46	6116	7309	11256	10915
248825	IPG	Kexin	3.4.21.61	PM/MT	protein binding	membrane		S	9.3135,79	28061	16731	49118	46496
293601	IPG/1D/2D	Beta-1,6-galactan biosynthesis protein (KNH1)	N.A.	CWOB	unknown function	cell wall		S	6.0248,49	143081	14337	18002	16172
248522	1D/2D	Lactonohydrolase		CM	hydrolyase activity	membrane		S	6.6158,16	14547	7483	2248	1503
146995	IPG/1D/2D	Lentinan-degrading exo-beta-1,3-glucanase	N.A.	unknown process	unknown function	unknown compartment		S	5.2786,69	1989	19082	15029	13219
291511	IPG/1D/2D	Springtip/long chain base-responsive protein LSP1	N.A.	endocytosis	protein binding	cytoplasm		-	8.0763,39	271	165	136	17
305232	1D	Deuterolysin M35 metalloprotease	1.1.1.-	PM/MT	protein binding	unknown compartment		S	5.9159,97	11746	11537	25663	18916
305232	1D	Malate dehydrogenase	1.1.1.-	CM	dehydrogenase activity	cytoplasm		S	9.3468,94	4852	51612	36933	45902
326114	IPG/1D	NAD-malate dehydrogenase		CM	dehydrogenase activity	intracellular		S	5.33158,76	1972	18878	8536	7459
303590	IPG	GPI-anchored small secreted protein (MSSP)		unknown process	unknown function	unknown compartment		S	5.9710,43	1085	3817	36380	39207
305856	IPG/1D/2D	55 kDa immunogenic protein		unknown process	unknown function	unknown compartment		-	7.5374,48	22081	9752	6723	5413
146975	IPG	88 kDa immunoreactive mammo protein MP88		unknown process	unknown function	unknown compartment		-	8.9811,74	33013	18889	16889	27546
146889	IPG/2D	88 kDa immunoreactive mammo protein MP88		unknown process	unknown function	unknown compartment		-	8.7440,00	40920	33013	16889	27546
146995	IPG/1D/2D	88 kDa immunoreactive mammo protein MP88		unknown process	unknown function	unknown compartment		-	6.9843,59	21702	14686	46554	53098
147000	IPG/1D/2D	88 kDa immunoreactive mammo protein MP88		unknown process	unknown function	unknown compartment		-	9.5915,52	34696	14262	26324	28620
248634	IPG/1D/2D	88 kDa immunoreactive mammo protein MP88		unknown process	unknown function	unknown compartment		-	7.0506,28	8133	4373	7688	6816
184303	IPG	Predicted protein		unknown process	unknown protein	unknown compartment		-	5.8640,82	36875	49731	36866	36618
192730	IPG	Predicted protein		unknown process	unknown protein	unknown compartment		-	5.5135,81	14505	12092	10520	13454
292223	1D	Predicted protein		unknown process	unknown protein	unknown compartment		-	5.2575,07	8887	20465	36621	28736
292646	IPG/1D/2D	Predicted protein		unknown process	unknown protein	unknown compartment		M	4.88035,33	4108	3784	7250	6677

Table 1. Continued

protein ID	method	code*	description (annotations retrieved from UniProtKB, JGI manual, or JGI automatic)	SP/Inr	EC number	GO BP*	GO MF	GO CC	TargetP location*	Theor. pI/MW	FLM	Douglas fr ECM	P. Tricho ECM	P. delto ECM
293121	1D/2D	N.A.	Predicted protein			unknown process	unknown function	unknown compartment	I	6.54/45.57	17252	18294	20421	18350
293906	IPG	N.A.	Predicted protein			unknown protein	unknown protein	unknown protein	S	6.59/92.20	1449	3707	15855	14686
294094	2D	N.A.	Predicted protein			unknown protein	unknown protein	unknown protein	S	5.99/30.79	12223	7322	19612	18472
294150	IPG/1D/2D	N.A.	Predicted protein			unknown process	unknown function	unknown compartment	S	9.00/72.56	26466	40570	49673	48082
294237	IPG	N.A.	Predicted protein			unknown protein	unknown protein	unknown protein	I	9.20/60.59	14225	7947	6887	5660
294358	IPG	N.A.	Predicted protein			unknown protein	unknown protein	unknown protein	I	5.68/59.55	5452	3517	2199	2832
295057	1D	N.A.	Predicted protein			unknown process	unknown function	unknown compartment	S	9.82/35.34	1270	2469	7707	5641
295080	IPG/1D	N.A.	Predicted protein			unknown process	unknown function	unknown compartment	S	5.33/62.36	8936	11874	13052	12781
297470	1D	N.A.	Predicted protein			unknown protein	unknown protein	unknown protein	I	9.02/42.73	4620	15535	45121	46933
297653	IPG	N.A.	Predicted protein			unknown protein	unknown protein	unknown protein	I	9.02/67.81	2782	14393	20927	19301
300910	IPG	N.A.	Predicted protein			unknown protein	unknown protein	unknown protein	S	6.78/140.91	9542	18765	25811	28738
301101	IPG	N.A.	Predicted protein			unknown protein	unknown protein	unknown protein	I	9.22/84.93	11864	24226	22887	22020
301770	IPG	N.A.	Predicted protein			unknown protein	unknown protein	unknown protein	I	9.89/88.12	19341	12015	8387	5358
304800	IPG	N.A.	Predicted protein			unknown protein	unknown protein	unknown protein	I	8.67/39.35	3305	2818	11961	7659
306233	ID	N.A.	Predicted protein			unknown protein	unknown protein	unknown protein	S	5.31/240.64	680	59801	61185	55586
306988	IPG	N.A.	Predicted protein			unknown protein	unknown protein	unknown protein	M	5.99/90.58	1	1	1	1
310871	IPG	N.A.	Predicted protein			unknown protein	unknown protein	unknown protein	S	7.59/66.47	27628	16173	38356	34849
312067	IPG/2D	N.A.	Predicted protein			unknown process	unknown function	unknown compartment	S	6.44/103.31	15190	5698	23907	20272
316624	IPG	N.A.	Predicted protein			unknown protein	unknown protein	unknown protein	S	4.89/36.77	36361	25475	42867	43975
318970	IPG	N.A.	Predicted protein			unknown protein	unknown protein	unknown protein	I	5.74/46.41	14567	53197	53175	59662
322658	IPG/1D/2D	N.A.	Predicted protein			unknown process	unknown function	unknown compartment	S	5.20/32.91	13490	3574	2010	1628
329947	IPG	N.A.	Predicted protein			unknown protein	unknown protein	unknown protein	S	4.96/61.67	113	443	210	380
332846	1D	N.A.	Predicted protein			unknown protein	unknown protein	unknown protein	S	9.12/66.47	173	731	178	285
333609	IPG	N.A.	Predicted protein			unknown protein	unknown protein	unknown protein	S	5.43/45.40	34	56	49	89
335948	2D	N.A.	Predicted protein			unknown protein	unknown protein	unknown protein	S	8.35/65.11	331	2800	852	894
295832	IPG	NAQHT	Ectomyomritza up-regulated Nach2-containing protein			unknown process	unknown function	unknown compartment	S	6.74/62.39	410	312	175	32
180699	ID	NLP3	Nuclease PA3		N.A.	unknown process	hydrolyase activity	unknown compartment	S	8.62/35.09	1466	5965	20219	18719
163800	IPG	PBL	Peptidocyan-binding LysM			unknown process	unknown function	membrane	S	4.17/11.23				
188879	IPG	PDI	Protein disulfide isomerase		5.3.4.1	PMM/IT	isomerase activity	membrane	S	5.45/71.32				
305002	IPG	PDI	Protein disulfide isomerase		5.3.4.1	PMM/IT	isomerase activity	membrane	S	6.94/32.98	5715	3068	7985	8236
295057	ID	PEPS	Pepsin A		3.4.23.1	PMM/IT	protein binding	cytoplasm	S	7.60/45.14	786	1129	712	683
309101	1D/2D	PEP1a	Aspartic peptidase A1		3.4.23.1	PMM/IT	protein binding	cytoplasm	S	8.90/60.42	51471	28433	32896	35020
291381	IPG	PEP1c	Subtilisin-like serine protease pepC		3.4.23.-	PMM/IT	protein binding	intracellular	S	5.75/29.79	24423	20672	38442	37066
293536	IPG/1D/2D	PEPTn	NpCP60-like cell-wall peptidase		N.A.	unknown process	unknown function	unknown compartment	S	5.15/29.45	11328	478	11858	22568
292054	1D/2D	PEPTs	Peptidase S10, serine carboxypeptidase		3.4.16.-	PMM/IT	protein binding	intracellular	S	7.53/161.77	6446	1902	303	179
306773	IPG/1D	PERI	Lipid droplet-associated perilipin protein			unknown process	unknown function	unknown compartment	I	6.15/78.54	3874	27179	26339	26515
188015	IPG	PERM	Amino acid permease-associated region			unknown process	protein binding	unknown compartment	I	10.78/6.52	34078	24835	17392	23302
293971	IPG	PGD2	Phosphogluconate 2-dehydrogenase		1.1.1.43	CM	dehydrogenase activity	cytoplasm	I	9.18/24.11	14970	22493	14009	17935
189339	IPG/2D	PGK	Phosphoglycerate kinase		2.7.2.3	CM	ATP binding	cytoplasm	I	6.40/61.67	16678	25930	10018	13535
305339	ID	PGM	Phosphoglucomutase		5.4.2.2	glycogen biosynthesis	protein binding	cytoplasm	I	10.09/70.57	1264	1758	799	1118
310810	1D/2D	PHOa	Acid phosphatase		3.1.3.2	phosphate metabolism	phosphatase activity	extracellular	S	9.32/20.66	4545	2885	1531	1605
142568	1D/2D	PHYA	Phytase		3.1.3.8	endocytosis	hydrolyase activity	extracellular	S	11.55/17.88	41228	32284	19447	25684
322816	IPG	PP2c	Protein phosphatase 2C		3.1.3.16	signal transduction	protein binding	cytoplasm	I	5.97/66.03	25701	23782	17794	1912
175463	ID	PP1A	Peptidyl-prolyl cis-trans isomerase		5.2.1.8	PMM/IT	phospholipase activity	intracellular	I	4.35/26.83	627	7311	7486	8274
145571	ID	PPLC	Protein phospholipase C, catalytic domain		6.3.2.19	PMM/IT	signal transduction	intracellular	I	10.49/34.86	30472	36365	39698	37058
192587	IPG	PR6	Thaumatin-like protein			response to stress	unknown function	extracellular	S	6.75/65.08	50065	29155	30015	29593
192602	ID	PRO1B	Profilin-1b			CCOOB	actin binding	intracellular	S	9.21/64.31	18685	18797	9270	12108
292104	2D	PRP	Proline-rich protein			unknown process	protein binding	cytoplasm	I	5.95/70.40	38090	35469	30551	47855
189695	ID	PR57	26S proteasome subunit P45		1.11.1.15	response to stress	antioxidant activity	mitochondrion	I	5.06/33.05	2636	6651	11354	11119
172963	IPG	PRX6	Peroxiredoxin-6		6.3.2.19	PMM/IT	protein binding	golgi apparatus	I	9.22/31.50	39062	38104	28606	28669
247319	IPG	PUB1	Ubiquitin-protein ligase PUB1		N.A.	ion transport	oxidoreductase activity	membrane	I	5.14/724.90	14888	418	127	1
185266	IPG	QOXR	NADH-quinone oxidoreductase		N.A.	signal transduction	oxidoreductase activity	membrane	I	9.07/26.51	15385	8295	6269	6545
190833	2D	QOXR	NADH-quinone oxidoreductase		N.A.	ion transport	oxidoreductase activity	membrane	I	9.24/66.79	36941	18061	16564	19943
306569	IPG/1D	RGa8	Rho-GTPase-activating protein 8			signal transduction	protein binding	unknown compartment	S	8.79/6.01	5315	5419	17677	21318
178618	IPG	RL4B	Ribosomal protein L4L1e			PMM/IT	RNA binding	intracellular	M	6.22/31.77	54891	51036	52221	48406
229443	IPG/1D	RLA2	Ribosomal protein L6S			PMM/IT	RNA binding	intracellular	I	6.79/6.01	5315	5419	17677	21318
306030	IPG/1D/2D	RLPA	Rare lipoprotein A (RlpA)			unknown process	unknown function	membrane	S	11.71/21.24	5281	8851	35955	36332
292975	IPG	RNP1	RNA-binding region RNP-1			RNAP/IT	RNA binding	nucleus	I	5.40/93.20	33530	28553	35407	34725
292573	ID	RS21	Ribosomal protein S21e			PMM/IT	RNA binding	intracellular	I	5.27/4.84	39726	29087	33685	38439
192584	IPG	RS3	Ribosomal protein S3			PMM/IT	RNA binding	intracellular	I					

Table 1. Continued

protein ID	method	code ^a	description (annotations retrieved from UniProtKB, JGI manual, or JGI automatic)	SP/nr	E.C. number	GO BP ^b	GO MF	GO CC	TargetP location ^c	Theor. pI/MW	FLM fir ECM	P. Tricho ECM	P. delta ECM
191565	IPG	SAR1	GTP-binding protein SAR1			PM1TT	protein binding	endoplasmic reticulum	S	5.6621.41			
192726	IPG	SKP1	Suppressor of kinetochore protein 1			PM1TT	protein binding	nucleus	-	N.A.	36872	48174	49089
311738	IPG	SLA1	Actin cytoskeleton-regulatory complex protein sla1			COCCOB	actin binding	intracellular	-	4.4014.18	8987	12275	8018
303799	2D	SOD	Superoxide dismutase	1.15.1.1		response to stress	antioxidant activity	intracellular	S	9.193.95	6794	40102	47815
185531	IPG	SPT4	Transcription initiation Spt4			RNAPMT	RNA binding	nucleus	-	9.0165.36	6248	10372	18678
190777	IPG	SSP	Small Secreted Protein			unknown protein	unknown protein	unknown protein	-	7.9711.30	786	2860	8799
192705	IPG	SSP	Small Secreted Protein			unknown protein	unknown protein	unknown protein	-	8.9818.90	20521	22436	20621
234095	IPG	SSP	Small Secreted Protein			unknown protein	unknown protein	unknown protein	-	9.5329.35	41607	34854	35955
292021	IPG/1D/2D	SSP	Small Secreted Protein			unknown process	unknown function	unknown compartment	S	5.129.66	46045	24795	21499
292425	IPG/1D	SSP	Small Secreted Protein			unknown process	unknown function	unknown compartment	S	8.7914.09	14228	53455	53119
292441	1D/2D	SSP	Small Secreted Protein			unknown process	unknown function	unknown compartment	S	10.2927.88	6240	18919	56803
293845	ID	SSP	Small Secreted Protein			unknown protein	unknown protein	unknown protein	S	10.119.15	32345	22004	28258
294567	IPG	SSP	Small Secreted Protein			unknown protein	unknown protein	unknown protein	-	4.3419.12	1892	8745	18660
294585	IPG	SSP	Small Secreted Protein			unknown protein	unknown protein	unknown protein	-	5.7718.73	6084	6203	12604
294686	IPG/1D	SSP	Small Secreted Protein			unknown process	unknown function	unknown compartment	S	4.8226.29	59823	7293	10369
295296	IPG/1D/2D	SSP	Small Secreted Protein			unknown process	unknown function	unknown compartment	S	10.7415.08	15607	1764	1878
295588	IPG	SSP	Small Secreted Protein			unknown process	unknown function	unknown compartment	S	4.8847.80	2954	13558	36307
295676	IPG/1D/2D	SSP	Small Secreted Protein			unknown process	unknown protein	unknown protein	S	8.637.28	43308	28763	57255
295742	IPG/1D/2D	SSP	Small Secreted Protein			unknown process	unknown function	unknown compartment	S	4.6016.19	9117	854	672
306974	IPG	SSP	Small Secreted Protein			unknown process	unknown function	unknown compartment	S	9.1024.88	32482	5432	7921
314526	IPG	SSP	Small Secreted Protein			unknown protein	unknown protein	unknown protein	S	6.566.95	7884	16188	18756
316820	ID	SSP	Small Secreted Protein			unknown protein	unknown protein	unknown protein	S	6.0523.17	39482	11524	10395
317006	IPG	SSP	Small Secreted Protein			unknown protein	unknown protein	unknown protein	S	9.1918.80	8649	6090	6941
318247	IPG/1D	SSP	Small Secreted Protein			unknown process	unknown function	unknown compartment	-	9.5818.84	4384	6995	8402
318310	IPG	SSP	Small Secreted Protein			unknown protein	unknown protein	unknown protein	-	4.6520.79	43376	35587	21027
319046	ID	SSP	Small Secreted Protein			unknown protein	unknown protein	unknown protein	S	11.5218.59	4840	19395	22342
322637	IPG	SSP	Small Secreted Protein			unknown protein	unknown protein	unknown protein	S	7.7625.82	49353	33001	28013
330228	IPG	SSP	Small Secreted Protein			unknown protein	unknown protein	unknown protein	-	4.4611.97	1243	1433	7348
187174	2D	STPP	Ser/Thr protein phosphatase family protein	N.A.		lipid metabolism	hydrolyase activity	unknown protein	S	9.1025.57	2217	2136	4452
315964	IPG	STPP42	S/T-protein phosphatase 4 regulatory subunit 2	N.A.		unknown process	protein binding	nucleus	M	6.26114.96	8501	7290	7553
248359	IPG/1D/2D	TAL1	Transaldolase	2.2.1.2		CM	transerase activity	cytoplasm	-	4.7930.59	17845	20595	23866
315910	IPG	TKL	Transketolase	2.2.1.1		CM	protein binding	intracellular	-	5.2424.75	45997	44789	32671
176780	2D	TPM	Tropomyosin	3.4.14.9		COCCOB	actin binding	cytoplasm	-	5.9554.44	21739	33304	30507
191088	IPG/1D/2D	TPP1	Tripeptidyl-peptidase 1			PM1TT	protein binding	intracellular	S	5.3737.90	4395	3815	3048
165781	IPG	TPR	TPR repeat			unknown process	unknown function	intracellular	-	9.8713.91			
181679	IPG/1D/2D	TRX	Thioredoxin	N.A.		electron transport	electron carrier activity	cytoplasm	-	6.8731.86	24454	34165	24841
295142	IPG/1D/2D	TRX	Thioredoxin	N.A.		electron transport	electron carrier activity	cytoplasm	-	10.746.32	18888	27906	36573
295143	1D/2D	TRX	Thioredoxin	N.A.		electron transport	electron carrier activity	cytoplasm	-	5.4182.77	9995	1941	1709
295069	IPG/1D	TYR	Tyrosinase	1.10.3.1		cell proliferation	protein binding	cytoplasm	M	5.8102.46	52502	51767	44595
186716	IPG/1D/2D	UBI1	Ubiquitin			PM1TT	protein binding	nucleus	-	5.4463.02	23954	33327	44115
192623	IPG/1D/2D	UBI2	Ubiquitin			PM1TT	protein binding	nucleus	-	7.9212.70	17526	28252	44104
234612	IPG/1D/2D	UBI3	Ubiquitin			PM1TT	protein binding	nucleus	-	5.3128.00	34580	32756	31425
290725	IPG/1D/2D	UBI4	Ubiquitin			PM1TT	protein binding	nucleus	-	9.6638.87	21570	14043	18807
309035	IPG/1D	VIP1	Protein VIP1 (diphosphoinositol-pentakisP kinase)	2.7.4.24		COCCOB	ATP binding	cytoplasm	-	4.7946.35	37486	41436	27607
184762	IPG	YI156	Uncharacterized protein yil156w-b			unknown process	unknown function	unknown compartment	S	6.717.43	9742	13344	16428
295794	IPG/1D	YOP1	Protein YOP1			PM1TT	protein binding	golgi apparatus	-	4.8860.10	37473	43049	42418
322030	IPG	ZnDCP	Zn-finger domain-containing protein			unknown process	unknown function	unknown compartment	M	6.5022.47	1619	2151	3600

^a code abbreviation: N.A. Not Available. ^b GO BP abbreviations: CWOB, cell wall organization and biogenesis; COCCOB, cytoskeleton and cellular component organization and biogenesis; CM, glycolysis, tricarboxylic acid cycle, pentose-phosphate shunt and carbohydrate metabolism; PM1TT, protein modification, metabolism, transport and translation; RNAPMT, RNA processing, metabolism and transcription. ^c TargetP abbreviations: M, mitochondrial location, S, extracellular location; -, other location.

database searching. The high confidence limit settings that were used in the analysis of peptide data, together with the identification of multiple peptides for most proteins, allowed for unambiguous identification of *L. bicolor* proteins.

3.2. Protein Identification from Secretome Samples

Three complementary proteomic methods were used to identify secreted proteins released by *L. bicolor* free-living mycelium in the growth medium: IPG shotgun, SDS-PAGE shotgun and 2-DE-MS/MS (Figure 1).

A total of 524 proteins were identified using IPG shotgun, across all 40 fractions, though this accounted for only 142 unique accessions when duplicates are removed (Supplementary Table S1, Supporting Information). On average, 13 proteins were identified *per* IPG shotgun fraction. Two proteins (accessions ID292021, an unknown protein, and ID305896, annotated as a 55 kDa immunogenic protein, Table 1) almost covered the whole length of the strip. An ectomycorrhiza up-regulated NACHT-containing protein (NACHT, ID 295832) was only identified using the IPG-IEF shotgun method.

The SDS-PAGE shotgun method identified 263 proteins corresponding to 116 unique accessions in the *L. bicolor* gene repertoire (Supplementary Table S1, Supporting Information). A 88 kDa mannoprotein (MP88, ID147000) was found in 13 out of 16 fractions.

Using 2-DE, a total of 210, 537 and 48 2-D spots were detected along 3–11, 4–7 and 7–11NL gradients, respectively (Supplementary Figure S2D, Supporting Information). The 201 spots excised for MS analyses yielded 267 proteins, corresponding to 77 unique accessions in the *L. bicolor* genome. Accession ID314722 was identified in 47 distinct spots, probably corresponding to post-translational forms of the same proteins which is a common feature of 2-DE. This protein was identified across the three proteomic methods and corresponded to a glucoglycosaminoglycan oxidase (GOOX). GOOX was also identified in mycelial samples. Enolase and GAPDH were also identified in culture filtrates. These proteins are not predicted to be secreted, and therefore likely to be intracellular contaminants resulting from mycelium lysis.

3.3. Comparison of the Three Proteomic Methods

Table 1 lists all 224 unique proteins identified from *L. bicolor* secretome samples using the three proteomic approaches, IPG-IEF shotgun, SDS-PAGE shotgun and 2-DE MS/MS, which identified 142, 116, and 77 unique proteins, respectively. Additional information can be found in the Supporting Information. Identified proteins were further annotated by retrieving Gene Ontology (GO) terms, Biological Process (BP), Molecular Function (MF), and Cellular Component (CC). Figure 2 and Supplementary Table S2 (Supporting Information) compare GO classifications for each method (“IPG”, “1-D” and “2-D”) as well as the combination of all of them (“all”). A significant proportion of identified proteins remained unclassified as they code for products involved in an unknown process (22%, 50/224 proteins), function (21%, 46/224 proteins) or compartment (27%, 61/224 proteins). The IPG-IEF shotgun method yielded the greatest proportion of unknown/unclassified proteins (49%). One of these novel putative secreted proteins of unknown function is a MiSSP (ID303550, 10.4 kD), that is, a protein of <300AA whose gene is induced in the symbiotic tissues. It is worth noting that GO and CC annotations were partly inaccurate as only 25 proteins out of 224 (11%) were predicted to be secreted (11 proteins in “Cell wall” and 14 proteins in “Extracellular”

compartments). TargetP prediction allocated 42% (95/224) of the proteins to the secretory pathway. GO CC annotation helped recover two proteins (a phytase and a clitocypin cysteine proteinase inhibitor) that had escaped TargetP predictions. NlpC/P60-like cell-wall peptidase and the five MP88s were altogether missed, thus emphasizing the limitation of automated gene predictions. Based on this functional annotation, the total number of proteins secreted in the growth medium was 103 (46%).

3.4. Increased Coverage of the *L. bicolor* Secretome

A Venn diagram shows the gain achieved by using combined proteomics approaches (Figure 3 and Supplementary Table S2, Supporting Information). Out of the 224 identified proteins, 36 were identified using all three methods, 7 proteins were common between IPG-IEF fractions and 2-D spots, 14 proteins were common between IPG-IEF fractions and SDS-PAGE fractions, and 18 proteins were common between SDS-PAGE fractions and 2-DE gel spots. Many proteins were only identified using a single technique; 85 proteins were only identified by IPG-IEF shotgun, whereas 49 proteins were only detected by SDS-PAGE, and 16 proteins were only found by 2-DE. To link these numbers to protein functions, the GO categories specific to one particular method or shared between several approaches have been added to the Venn diagram, as well as some of the protein isoforms. We will not discuss all of the GO categories displayed in Figure 3 but provide a few examples that illustrate the advantage of combining various electrophoresis techniques.

All five isoforms of the 20 kD heat shock protein (HSP20) were exclusively identified in SDS-PAGE fractions. The two glycosyltransferases (GT8 and GT69) and both protein disulfide isomerases (PDI) identified in this work were exclusively found in IPG-IEF fractions. All of the glycosylphosphatidylinositol (GPI)-small secreted proteins (GPI-SSP) were only observed using shotgun methods, not 2-DE. All three GPI-phospholipase C (GPI-PLC) isoforms were observed in SDS-PAGE fractions and 2-D spots, not in IPG-IEF fractions. Some proteins involved in lipid metabolism were uniquely detected by the 2-DE method, and none of the proteins identified using the IPG-IEF shotgun method belonged to the “Phosphatase activity” MF category. Some proteins (expansin, two GH17 glucan 1,3-beta-glucosidases, GH16 endo-1,3(4)-beta-glucanase) belonging to “Cell wall” CC and “Cell wall organisation and biogenesis” BP categories were exclusively identified using the SDS-PAGE method. Likewise, other proteins [protein phosphatase 2C (PP2c), and calnexin (CALX)] belonging to “Endoplasmic reticulum (ER)” CC were exclusively identified using the IPG-IEF shotgun method. Again, these observations highlight the need to combine various analytical approaches to identify as many proteins as possible in a given sample.

3.5. Transcript Profiling

Out of the 224 identified secreted proteins, 93% (210/224 proteins) have a detectable transcript in the microarray profiling (Table 1), most of which presenting significant fold-changes in the ECM roots of Douglas fir, *P. trichocarpa* and/or *P. deltooides* relative to their abundance in FLM (Table 2). Many (53/210, 25%) were of unknown function, including the gene displaying the highest ECM/FLM induction ratio (ID305233), being 75- to 80-fold more expressed in ECM than in FLM. Of particular interest are the nine induced genes encoding small secreted proteins (ID306974, ID294585, ID292425, ID318310, ID322637, ID292441, ID294567, ID295296, and ID190777), likely involved in symbiosis and potentially including MiSSPs. Other highly induced genes, particularly in ECM roots of poplar species,

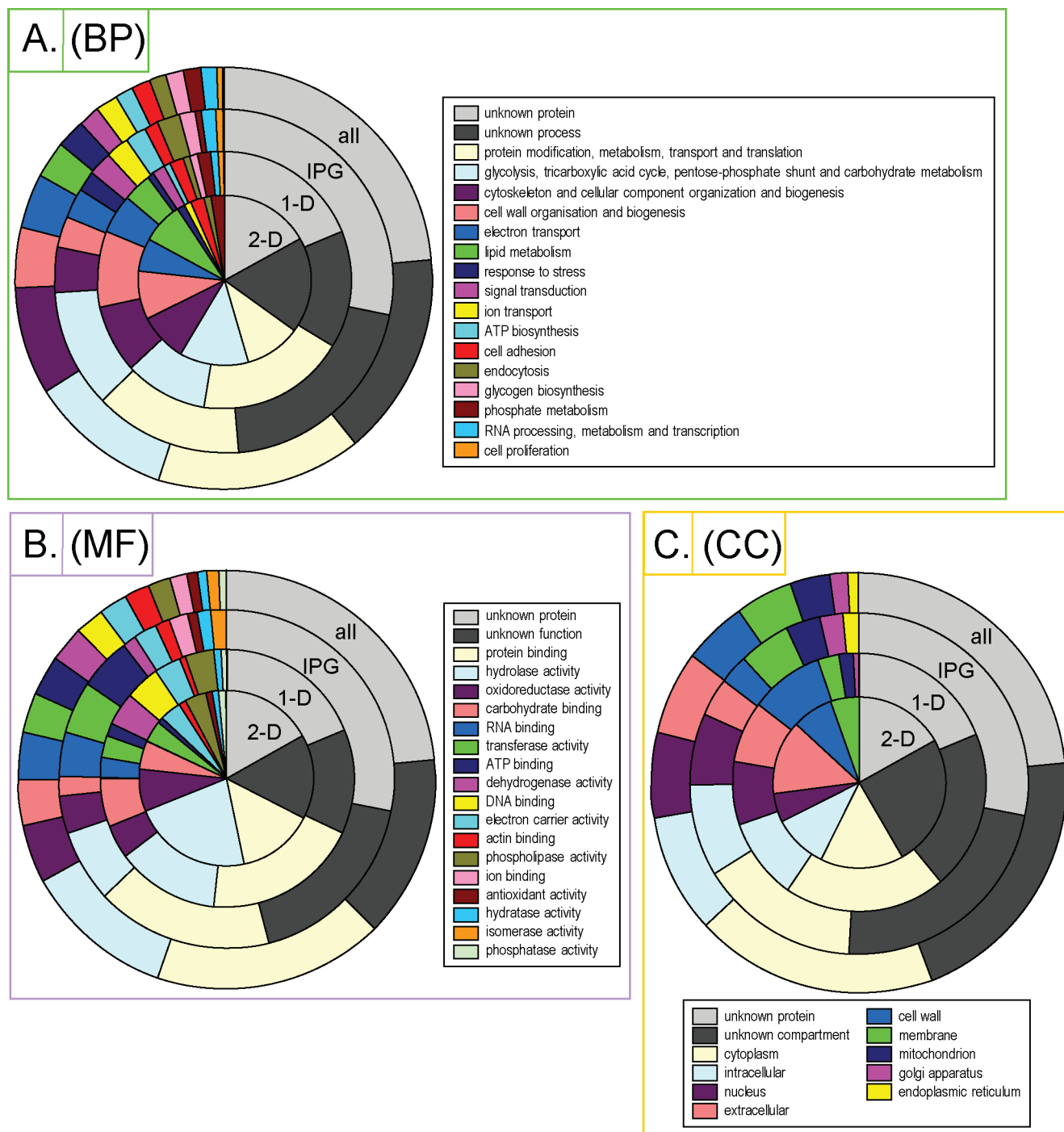


Figure 2. Gene Ontology (GO) classification of *L. bicolor* identified secreted proteins using 2-DE (2-D), 1-D shotgun (1-D), IPG shotgun (IPG) or all three techniques (all), according to (A) biological process (BP), (B) molecular function (MF), and (C) cellular component (CC).

included a putative ARF GTPase activator (ID310440), a 55 kDa immunogenic protein (ID305896), and a gene encoding for a small secreted protein (ID190777) (Table 1). The expression of some genes seemed to be host-specific. For instance, a heat shock protein of 20 kD (ID235684) was 8.4-time induced in ECM roots of *P. deltoides* only and a GPI-SSP (ID335186) almost 3-time induced in ECM roots of Douglas fir only (Table 1). Overall, the genes displaying fold-change in ECM roots relative to FLM were found across all three species, and particularly the poplar species which displayed more consistency. Interestingly a gene encoding

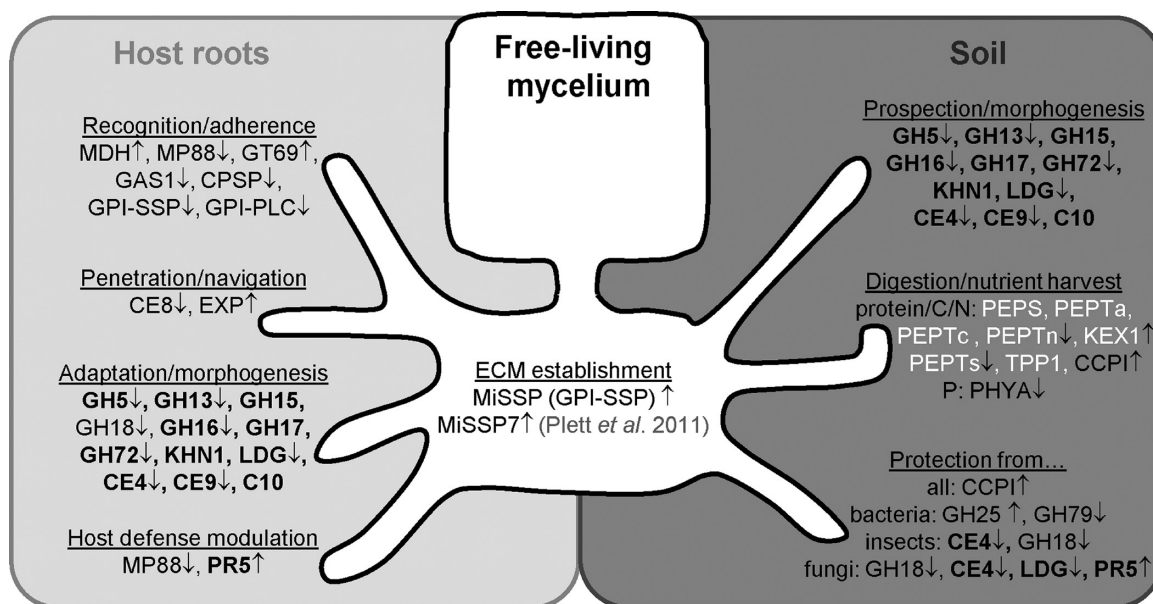
a superoxide dismutase (SOD, ID303799) presented a 5- to 7-fold induction in all ECM roots. Other antioxidant proteins, three thioredoxins (ID295143, ID181679, and ID295142) and one peroxiredoxin 6 (ID172363), were identified in the *L. bicolor* culture filtrate but not observed to be induced in ECM roots (Table 1).

4. DISCUSSION

This study describes the identification of the most abundant proteins from the mycelium of *L. bicolor* and those secreted into

Table 2. Number and Percentage (in brackets) of Transcript Displaying 2.0- or 2.5-Fold Changes in ECM Roots of Douglas fir, *P. trichocarpa* and *P. deltooides* Relative to Their Abundance in Free-living Mycelium (FLM)

	2.0-fold change		2.5-fold change	
	down-regulation (%)	up-regulation (%)	down-regulation (%)	up-regulation (%)
Douglas fir ECM/FLM ratio	45 (21.5%)	31 (14.8%)	30 (14.4%)	25 (12.0%)
<i>P. trichocarpa</i> ECM/FLM ratio	57 (27.3%)	48 (23.0%)	40 (19.1%)	41 (19.6%)
<i>P. deltooides</i> ECM/FLM ratio	47 (22.5%)	49 (23.4%)	40 (19.1%)	44 (21.1%)

**Figure 4.** Working model of *L. bicolor* mode-of-action to establish its biotrophic and saprophytic lifestyles based on experimental proteomic results. The full names of the proteins are indicated in Table 1. Ambiguous secreted proteins that cannot be specifically ascribed to one lifestyle in particular are in bold letters. Proteases are in white. Significant fold-changes of gene expression in the ECM roots of Douglas fir, *P. trichocarpa* and/or *P. deltooides* relative to their abundance in FLM are represented by arrows facing up or down which correspond to up- and down-regulated transcript levels, respectively. C, carbon; N, nitrogen; P, phosphorus.

in secretome samples and was annotated as a glycosylphosphatidylinositol (GPI)-anchored protein inserted in the plasma membrane, suggesting that it remains within the cell wall. This MiSSP (ID303550) was reported to be at least 10 times induced in ECM roots of two poplar species.⁸ Most of these secreted proteins (93/103, 90%) were predicted to be involved in symbiosis based on the transcript profiling carried out on both FLM and ECM roots (Table 1).

The following sections attempt to ascribe to qualitatively identified secreted proteins, substantiated by quantitative gene expression data, a particular mode-of-action of the ECM fungus (Figure 4). Although a causal link can be drawn between symbiosis and a gene up-regulated in ECM roots, the consideration of down-regulated genes is equally informative as they are also biomarkers of symbiosis establishment. In this study, all significantly differentially expressed genes are deemed involved in *L. bicolor* mode-of-action.

4.1. Saprotrophic Lifestyle at the Root–Soil Interface

The fungal CW is a complex glycoprotein- and polysaccharide-based three-dimensional network. Polysaccharides (90% of the CW) consist of branched beta-1,3/1,6-glucans linked to chitin via beta-1,4 linkages, and glycoproteins. Ten percents of

the CW include mannoproteins and GPI-anchored proteins.²⁸ Many carbohydrate-active-enzymes (CAZymes) were identified in secretome of *L. bicolor*, most of them transcriptionally down-regulated with the exception of one GH15 (ID295790) which was consistently highly up-regulated in all ECM roots (Table 1). These CAZymes are likely involved in CW polysaccharide modification, along with KNH1, a protein involved in beta-1,6-glucan biosynthesis, and a lentinan-degrading exobeta-1,3-glucanase (LDG) that hydrolyses a fungal CW component. Most of the GHs identified in this study act on glucan moieties (GH5, GH13, GH15, GH16, GH17, GH72, GH79, KNH1, and LDG). Chitinase (GH18) and endobeta-1,3 glucanases (GH16, GH17) are required for mycelial cell separation due to the presence of chitin in the primary septum and beta-glucan in the secondary septum.²⁸ Several members of carbohydrate esterases were also identified in *L. bicolor* secretome (6 CE4s, 1 CE8, 1 CE9, and 3 CE10s). Chitin deacetylases (CE4) modify chitin in the less rigid deacetylated chitosan. *N*-Acetylglucosamine-6-phosphate deacetylase (CE9) catalyzes the hydrolysis of the acetamido groups of *N*-acetylglucosamine residues in CW peptidoglycan.²⁸ We hypothesize that these CAZymes are mediating *L. bicolor* hyphal growth, as well as facilitating the morphogenic transition required when environmental (edaphic or host) conditions evolve.

Many extracellular proteases were identified in the *L. bicolor* culture filtrates: candidapepsin (CPEPS), pepsin A (PEPS), aspartic peptidase A1 (PEPTa), (carboxy)peptidase S10 (PEPTs), NlpC/P60-like cell-wall peptidase (PEPTn), tripeptidyl-peptidase 1 (TPP1), kexin (KEX1), and subtilisin-like serine protease pepC (PEPTc). KEX1 was transcriptionally induced in ECM roots while the PEPTn and PEPTs were down-regulated (Table 1). Other aspartic peptidase/pepsin (A01A) and subtilisin (S08A) proteases were differentially regulated during ECM and fruiting body development.⁸ Aspartic proteases are active at acidic pHs and the basidiomycete *A. muscaria* secretes two aspartic proteases that mediate nitrogen acquisition from protein-containing organic matter.²⁹ The large set of proteases constitutively secreted by *L. bicolor* in the absence of protein sources in the medium suggests that *L. bicolor* relies on the action of extracellular peptidases to either finalise maturing of secreted proteins or/and degrade proteins present in the soil decomposing materials to retrieve nitrogen, phosphorus, and to a lesser extent carbon, during its transitory saprotrophic phase. Peptidases are inactivated by type-specific small molecule inhibitors that are critical for maintaining the peptidase-antipeptidase balance in all living organisms. Clitocypin is an extracellular cysteine proteinase inhibitor that was purified from fruiting bodies of the basidiomycete *Clitocybe nebularis*.³⁰ Clitocypin inhibits papain, another secreted protease of *L. bicolor*,⁸ but is inactive toward pepsin.³⁰ Transcript abundance of two genes encoding for clitocypin cysteine proteinase inhibitor (CCPI) was very high in ECM roots (minimum of 16-fold change, Table 1) and fruiting bodies of *L. bicolor*;⁸ our study indicates that the protein is extracellular. Being active with some of the peptidases secreted by *L. bicolor*, this inhibitor could play a role in physiological endogenous regulation of the extracellular proteolytic activities of the fungus.

A phytase (PHYA) was also identified in the medium filtrate and was transcriptionally down-regulated in ECM roots (Table 1). Under symbiosis, *L. bicolor* is likely to resort to phytase which would be secreted by the exploring hyphae to use phosphorus from the soil and redirect it to its host and other parts of the mycelial colony.

4.2. Protection against Pathogens and Predators

While prospecting the soil to harvest nutrients, hyphae encounter various rhizospheric micro-organisms. They can be parasites such as chitinolytic bacteria and pathogenic fungi, or animals feeding off of the mycelium such as grazing nematodes, or competitors for the same niche. *L. bicolor* could limit bacterial attacks by using secreted GH25 and GH79. The lysozyme GH25 was consistently transcriptionally up-regulated in ECM roots (from 1.7 to 4.4 fold change, Table 1). Also known as muramidase, GH25 acts on bacterial CW by catalyzing the hydrolysis of 1,4-beta-linkages between N-acetylmuramic acid and N-acetyl-D-glucosamine residues in a peptidoglycan. Three beta-glycan active enzymes (GH79) were identified in *L. bicolor* secretome, with two of them found to be transcriptionally down-regulated in ECM roots (ID295325 and ID295469, Table 1). The latter present putative beta-glucuronidase activity on fungal or plant beta-glycans while the third GH79 (ID184692) also displays a putative hyaluronidase activity, possibly by hydrolyzing polysaccharides outside fungal and plant kingdoms (Veneault-Fourrey C., Pers. comm.). To date, only one family of GH79 has been characterized in fungi; beta-glucuronidases from *Aspergillus niger* and *Neurospora crassa* hydrolyze the carbohydrate moieties of arabinogalactan-proteins,³¹ thus potentially impairing the

function of proteoglycans in higher plants. Although the role of these enzymes remains unclear, the GH79 family was associated with defense against bacterial pathogens.⁸ Protection against fungal pathogens could also be mediated by the thaumatin-like protein (PR5), consistently highly induced in ECM roots (from 11.7 to 13.2-fold change, Table 1) and LDG, a fungal CW component.

4.3. Cell Wall-related Proteins

Four GPI-anchored small secreted proteins (GPI-SSPs) were identified in *L. bicolor* medium filtrates and two of them, ID292424 and ID335186, were respectively down- and up-regulated in ECM roots of Douglas fir (Table 1). A different member of this protein family (ID333839) was induced >14,000 times in ECM roots of poplar and Douglas fir relative to FLM,⁸ suggesting that these GPI-anchored proteins may play a role in the symbiotic interaction. Three GPI-specific phospholipase C proteins (GPI-PLC) were identified in the *L. bicolor* secretome, for which two (ID318365 and ID335698) showed no significant change in transcript abundance (Table 1). GPI-anchored proteins are involved in diverse cellular functions including cell adhesion, membrane trafficking, immune system signaling, and nutrient uptake;³² all of these roles may be involved in the symbiosis development.

Five mannoproteins (MP88) were identified in *L. bicolor* culture filtrates, most of them were down-regulated in ECM roots, except for ID146995, which was slightly induced in ECM roots of both poplar species (Table 1). MP88 features a C-terminal serine/threonine-rich region, possibly a site for extensive O-glycosylation, followed by a putative GPI anchor site.³³ CW mannoproteins enable specific cell–cell and cell–substrate interactions and the subsequent hyphae extension within the host or the soil.²⁸ Several mannoproteins are up-regulated in the *Pisolithus tinctorius-Eucalyptus globulus* ECM symbiosis.³⁴ Present in the *L. bicolor* secretome, the transcription of a GAS1-like mannoprotein was down-regulated in ECM roots of poplar and Douglas fir species (0.29–0.56-fold change, Table 1). Being generally repressed in our study, MP88 and GAS1-like mannoproteins might play a less active role in *L. bicolor* interaction with his host. Alpha-1,3-mannosyltransferase (GT69) adds the terminal mannose to the outer chain branches of N-linked mannan. It would therefore enable cell recognition events. GT69 transcript level increased in poplar ECM roots (2.7–3.0-fold change, Table 1). A cerato-platanin (CP)-related secreted protein (CPSP) was identified in *L. bicolor* secretome samples; it was transcriptionally down-regulated (0.20–0.54-fold change, Table 1). Like hydrophobins, CP proteins self-assemble into a surface coating involved in hyphae formation and adherence to surfaces.³⁵

4.4. Penetration of the Root Cortical Cells and Colonisation of the Apoplastic Space

L. bicolor lacks the enzyme repertoire to hydrolyze plant CW polysaccharides.⁸ The only plant CW-degrading enzyme identified in our study was a pectinesterase (CE8), a CW-associated protein that catalyzes the de-esterification of pectin, one of the main plant CW components, into pectate and methanol. An expansin (EXPN) was also identified in *L. bicolor* filtrates, and its transcript levels did not change in ECM roots (Table 1). *In planta*, EXPN may facilitate hyphae penetration into the root apoplastic space by loosening host cell walls,⁸ possibly with the joint activity of CE8 despite its down-regulation in ECM roots (Table 1).

5. CONCLUSIONS

In summary, the secretome of the free-living mycelium of *L. bicolor* was analyzed using several complementary proteomic approaches providing the first protein profiling of the secreted proteins for an ECM fungus. We identified a large repertoire of hydrolytic enzymes acting on CW polysaccharides and extracellular proteins. Most detected CAZymes are likely involved in the CW remodeling linked to hyphal growth, whereas secreted proteases may be used for digesting soil organic compounds and/or fending off competitors, pathogens and predators. A large fraction of the secreted proteins, including SSPs, have no known function but may be involved in the communication between hyphae or with the plant as recently shown for MiSSP7.¹²

As depicted in Figure 4, ECM fungi's dual lifestyle results in two different sets of proteins needed for different activities. On one hand, as free-living mycelium, *L. bicolor* requires proteins for hyphal prospection, adaptation to the soil environment via morphogenesis, digestion of decaying matter, nutrient harvest, and protection against pathogens and predators at the soil-fungus interface. On the other hand, when entering into symbiosis, it requires tools for recognition of the compatible host, adhesion to root surface, penetration of cortical cells, navigation through the apoplastic space, adaptation to the root environment via morphogenesis, and modulation of host defense mechanisms at the roots–fungus interface. A better insight into *L. bicolor*'s dual lifestyles would be gained from *in planta* proteomic studies.

■ ASSOCIATED CONTENT

Supporting Information

Supplementary tables, figures, methods, and results. This material is available free of charge via the Internet at <http://pubs.acs.org>.

■ AUTHOR INFORMATION

Corresponding Author

*Corresponding author: Dr. Delphine Vincent. Research School of Biology, RN Robertson Building (Bldg 46), The Australian National University, Canberra, ACT 0200 Australia. Phone: +61 2 61254026. Fax: +61 2 61254331. E-mail: comtasr@yahoo.fr.

■ ACKNOWLEDGMENT

We thank Pr. Marc Bonneu, in charge of the MS facility, as well as Anne-Marie Lomenech for her help with MS analyses. We also thank Dr Claire Veneault-Fourrey and Dr Krista Plett for careful reading of the manuscript. This project was funded by the Agence Nationale de la Recherche (project FungEffector, ANR-06-BLAN-0399) and Institut National de la Recherche Agronomique. This research was also sponsored by the Genomic Science Program of the US Department of Energy, Office of Science, Biological and Environmental Research under contract DE-AC05-00OR22725 (Plant-Microbe Interface).

■ REFERENCES

(1) Read, D. J.; Perez-Moreno, J. Mycorrhizas and nutrient cycling in ecosystems - A journey towards relevance? *New Phytol.* **2003**, *157* (3), 475–492.
 (2) Finlay, R.; Soderstrom, B. Mycorrhiza and carbon flow in the soil. In *Mycorrhizal Functioning: An Integrated Plant Fungal Process*; Allen, M. F., Ed.; Chapman and Hall: New York, 1992; pp 134–160.

(3) Felten, J.; Kohler, A.; Morin, E.; Bhalerao, R. P.; Palme, K.; Martin, F.; Ditengou, F. A.; Legue, V. The Ectomycorrhizal Fungus *Laccaria bicolor* Stimulates Lateral Root Formation in Poplar and Arabidopsis through Auxin Transport and Signaling. *Plant Physiol.* **2009**, *151* (4), 1991–2005.

(4) Martin, F.; Duplessis, S.; Ditengou, F.; Lagrange, H.; Voiblet, C.; Lapeyrie, F. Developmental cross talking in the ectomycorrhizal symbiosis: signals and communication genes. *New Phytol.* **2001**, *151* (1), 145–154.

(5) Peterson, R. L.; Bonfante, P. Comparative structure of vesicular-arbuscular mycorrhizas and ectomycorrhizas. *Plant Soil* **1994**, *159*, 79–88.

(6) Tagu, D.; Martin, F. Molecular analysis of cell wall proteins expressed during the early steps of ectomycorrhiza development. *New Phytol.* **1996**, *133* (1), 73–85.

(7) Dexheimer, J.; Pargney, J. C. Comparative anatomy of the host-fungus interface in mycorrhizas. *Experientia* **1991**, *47*, 312–320.

(8) Martin, F.; Aerts, A.; Ahren, D.; Brun, A.; Danchin, E. G.; Duchaussoy, F.; Gibon, J.; Kohler, A.; Lindquist, E.; Pereda, V.; Salamov, A.; Shapiro, H. J.; Wuyts, J.; Blaudez, D.; Buee, M.; Brokstein, P.; Canback, B.; Cohen, D.; Courty, P. E.; Coutinho, P. M.; Delaruelle, C.; Detter, J. C.; Deveau, A.; DiFazio, S.; Duplessis, S.; Fraissinet-Tachet, L.; Lucic, E.; Frey-Klett, P.; Fourrey, C.; Feussner, I.; Gay, G.; Grimwood, J.; Hoegger, P. J.; Jain, P.; Kilaru, S.; Labbe, J.; Lin, Y. C.; Legue, V.; Le Tacon, F.; Marmeisse, R.; Melayah, D.; Montanini, B.; Muratet, M.; Nehls, U.; Niculita-Hirzel, H.; Oudot-Le Secq, M. P.; Peter, M.; Quesneville, H.; Rajashekar, B.; Reich, M.; Rouhier, N.; Schmutz, J.; Yin, T.; Chalot, M.; Henrissat, B.; Kues, U.; Lucas, S.; Van de Peer, Y.; Podila, G. K.; Polle, A.; Pukkila, P. J.; Richardson, P. M.; Rouze, P.; Sanders, I. R.; Stajich, J. E.; Tunlid, A.; Tuskan, G.; Grigoriev, I. V. The genome of *Laccaria bicolor* provides insights into mycorrhizal symbiosis. *Nature* **2008**, *452* (7183), 88–92.

(9) Martin, F.; Kohler, A.; Murat, C.; Balestrini, R.; Coutinho, P. M.; Jaillon, O.; Montanini, B.; Morin, E.; Noel, B.; Percudani, R.; Porcel, B.; Rubini, A.; Amicucci, A.; Anselem, J.; Anthouard, V.; Arcioni, S.; Artiguenave, F.; Aury, J. M.; Ballario, P.; Bolchi, A.; Brenna, A.; Brun, A.; Buee, M.; Cantarel, B.; Chevalier, G.; Couloux, A.; Da Silva, C.; Denoed, F.; Duplessis, S.; Ghignone, S.; Hilselberger, B.; Iotti, M.; Marcais, B.; Mello, A.; Miranda, M.; Pacioni, G.; Quesneville, H.; Riccioni, C.; Ruotolo, R.; Splivallo, R.; Stocchi, V.; Tisserant, E.; Viscomi, A. R.; Zambonelli, A.; Zampieri, E.; Henrissat, B.; Lebrun, M. H.; Paolocci, F.; Bonfante, P.; Ottonello, S.; Wincker, P. Perigord black truffle genome uncovers evolutionary origins and mechanisms of symbiosis. *Nature* **2010**, *464* (7291), 1033–1038.

(10) Martin, F.; Selosse, M. A. The *Laccaria* genome: a symbiont blueprint decoded. *New Phytol.* **2008**, *180* (2), 296–310.

(11) Veneault-Fourrey, C.; Martin, F. Mutualistic interactions on a knife-edge between saprotrophy and pathogenesis. *Curr. Opin. Plant Biol.* **2011**, *14* (4), 444–450.

(12) Plett, J. M.; Kemppainen, M.; Kale, S. D.; Kohler, A.; Legue, V.; Brun, A.; Tyler, B. M.; Pardo, A.; Martin, F. A secreted effector protein of *Laccaria bicolor* is required for symbiosis development. *Curr. Biol.* **2011**, *21*, 1197–1203.

(13) Bouws, H.; Wattenberg, A.; Zorn, H. Fungal secretomes—nature's toolbox for white biotechnology. *Appl. Microbiol. Biotechnol.* **2008**, *80* (3), 381–388.

(14) Vincent, D.; Balesdent, M. H.; Gibon, J.; Claverol, S.; Lapailleur, D.; Lomenech, A. M.; Blaise, F. O.; Rouxel, T.; Martin, F.; Bonneu, M.; Anselem, J.; Dominguez, V.; Howlett, B. J.; Wincker, P.; Joets, J.; Lebrun, M. H.; Plomion, C. Hunting down fungal secretomes using liquid-phase IEF prior to high resolution 2-DE. *Electrophoresis* **2009**, *30* (23), 4118–4136.

(15) Di Battista, C.; Selosse, M. A.; Bouchard, D.; Strenstrom, E.; Le Tacon, F. Variations in symbiotic efficiency, phenotypic characters and ploidy level among different isolates of the ectomycorrhizal basidiomycete *Laccaria bicolor* strain S 238. *Mycol. Res.* **1996**, *100*, 1315–1324.

(16) Essader, A. S.; Cargile, B. J.; Bundy, J. L.; Stephenson, J. L., Jr A comparison of immobilized pH gradient isoelectric focusing and

strong-cation-exchange chromatography as a first dimension in shotgun proteomics. *Proteomics* **2005**, *5* (1), 24–34.

(17) Laemmli, U. K. Cleavage of structural proteins during the assembly of the head of bacteriophage T4. *Nature* **1970**, *227* (5259), 680–685.

(18) O'Farrell, P. H. High resolution two-dimensional electrophoresis of proteins. *J. Biol. Chem.* **1975**, *250* (10), 4007–4021.

(19) Ferry-Dumazet, H.; Houel, G.; Montalent, P.; Moreau, L.; Langella, O.; Negroni, L.; Vincent, D.; Lalanne, C.; de Daruvar, A.; Plomion, C.; Zivy, M.; Joets, J. PROTIcDb: a web-based application to store, track, query, and compare plant proteome data. *Proteomics* **2005**, *5* (8), 2069–2081.

(20) Gasteiger, E.; Gattiker, A.; Hoogland, C.; Ivanyi, I.; Appel, R. D.; Bairoch, A. ExPASy: The proteomics server for in-depth protein knowledge and analysis. *Nucleic Acids Res.* **2003**, *31* (13), 3784–3788.

(21) Emanuelsson, O.; Nielsen, H.; Brunak, S.; von Heijne, G. Predicting subcellular localization of proteins based on their N-terminal amino acid sequence. *J. Mol. Biol.* **2000**, *300* (4), 1005–1016.

(22) Altschul, S. F.; Gish, W.; Miller, W.; Myers, E. W.; Lipman, D. J. Basic local alignment search tool. *J. Mol. Biol.* **1990**, *215* (3), 403–410.

(23) Cantarel, B. L.; Coutinho, P. M.; Rancurel, C.; Bernard, T.; Lombard, V.; Henrissat, B. The Carbohydrate-Active EnZymes database (CAZy): an expert resource for Glycogenomics. *Nucleic Acids Res.* **2009**, *37* (Database issue), D233–238.

(24) Fraenkel, D. G. The top genes: on the distance from transcript to function in yeast glycolysis. *Curr. Opin. Microbiol.* **2003**, *6* (2), 198–201.

(25) Kiraga, J.; Mackiewicz, P.; Mackiewicz, D.; Kowalczyk, M.; Biecek, P.; Polak, N.; Smolarczyk, K.; Dudek, M. R.; Cebart, S. The relationships between the isoelectric point and: length of proteins, taxonomy and ecology of organisms. *BMC Genomics* **2007**, *8*, 163.

(26) Wu, S.; Wan, P.; Li, J.; Li, D.; Zhu, Y.; He, F. Multi-modality of pI distribution in whole proteome. *Proteomics* **2006**, *6* (2), 449–455.

(27) Santoni, V.; Rabilloud, T.; Doumas, P.; Rouquie, D.; Mansion, M.; Kieffer, S.; Garin, J.; Rossignol, M. Towards the recovery of hydrophobic proteins on two-dimensional electrophoresis gels. *Electrophoresis* **1999**, *20* (4–5), 705–711.

(28) Latgé, J. P. The cell wall: a carbohydrate armour for the fungal cell. *Mol. Microbiol.* **2007**, *66* (2), 279–290.

(29) Nehls, U.; Bock, A.; Einig, W.; Hampp, R. Excretion of two proteases by the ectomycorrhizal fungus *Amanita muscaria*. *Plant, Cell Environ.* **2001**, *24* (7), 741–747.

(30) Brzin, J.; Rogelj, B.; Popovic, T.; Strukelj, B.; Ritonja, A. Clitocyprin, a new type of cysteine proteinase inhibitor from fruit bodies of mushroom *clitocybe nebularis*. *J. Biol. Chem.* **2000**, *275* (26), 20104–20109.

(31) Konishi, T.; Kotake, T.; Soraya, D.; Matsuoka, K.; Koyama, T.; Kaneko, S.; Igarashi, K.; Samejima, M.; Tsumuraya, Y. Properties of family 79 beta-glucuronidases that hydrolyze beta-glucuronosyl and 4-O-methyl-beta-glucuronosyl residues of arabinogalactan-protein. *Carbohydr. Res.* **2008**, *343* (7), 1191–1201.

(32) Fujita, M.; Kinoshita, T. Structural remodeling of GPI anchors during biosynthesis and after attachment to proteins. *Febs Lett.* **2010**, *584* (9), 1670–1677.

(33) Huang, C.; Nong, S. H.; Mansour, M. K.; Specht, C. A.; Levitz, S. M. Purification and characterization of a second immunoreactive mannoprotein from *Cryptococcus neoformans* that stimulates T-Cell responses. *Infect. Immun.* **2002**, *70* (10), 5485–5493.

(34) Laurent, P.; Voiblet, C.; Tagu, D.; de Carvalho, D.; Nehls, U.; De Bellis, R.; Balestrini, R.; Bauw, G.; Bonfante, P.; Martin, F. A novel class of ectomycorrhiza-regulated cell wall polypeptides in *Pisolithus tinctorius*. *Mol. Plant-Microbe Interact.* **1999**, *12* (10), 862–871.

(35) Pazzagli, L.; Zoppi, C.; Carresi, L.; Tiribilli, B.; Sbrana, F.; Schiff, S.; Pertinhez, T. A.; Scala, A.; Cappugi, G. Characterization of ordered aggregates of cerato-platanin and their involvement in fungus-host interactions. *Biochim. Biophys. Acta* **2009**, *1790* (10), 1334–1344.